UDC 004.942

Y. Storozh, I. Lyutak, B. Storozh, O. Vasylyk, M. Yatsyshyn, M. Pasyeka

## Computer aided analysis of ball burnishing process

В рамках анализа процессов обкатывания шариком создана и исследована конечно-элементная модель вдавливания жесткой сферы в полупространство. Модель свидетельствует о высокой точности воспроизведения упругости материала по теории Герца. Изучено упруго-пластичное поведение материала со степенной зависимостью изотропного деформационного усиления. Обоснованы рекомендации выбора параметров исследования процесса обкатывания шариком.

**Ключевые слова**: конечно-элементный анализ, обкатывание шариками, упруго-пластичная деформация, упрочнение, конечно-элементная модель.

The finite element model analysis of a rigid sphere indentation into a half-space is created and investigated as a part of comprehensive study of a ball burnishing process. The model shows good fidelity of the material elastic behavior by the Hertz contact theory. The elastic-plastic behavior of the material with a power dependence of the isotropic strain strengthening is studied. Parameters for the further ball burnishing research are recommended.

**Keywords**: finite element analysis, burnishing, elastic-plastic deformation, strengthening, finite element model.

В межах аналізу процесів обкочування кулькою створено і досліджено скінченно-елементну модель вдавлювання жорсткої сфери в півпростір. Модель свідчить про високу точність відтворення пружної поведінки матеріалу за теорією Герца. Вивчено пружно-пластичну поведінку матеріалу зі степеневою залежністю ізотропного деформаційного зміцнення. Обгрунтовано рекомендації щодо вибору параметрів дослідження процесу обкочування кульками.

**Ключові слова:** скінчено-елементний аналіз, обкочування кульками, пружно-пластична деформація, зміцнення, скінченно-елементна модель.

**Introduction.** Burnishing is a cold working process in which plastic deformation occurs by applying a pressure through a ball or roller on the metallic surfaces. It is a finishing and strengthening process. Improvements in surface finish, surface hardness, wear resistance, fatigue resistance, yield and tensile strength, and corrosion resistance can be achieved by applying this process [1–3]. In addition, burnishing is a highly efficient, technological, and saving-cost process. It can be combined with cutting. Therefore, it is widely used in today's manufacturing industry for finishing enhanced machine parts.

However, despite more than 50-year period of the burnishing industrial application, numerous studying, and its seeming simplicity, till now there are not enough reliable engineering methods for predicting the surface layer quality suitable for manufacturing process planning to produce products with predetermined properties. An empirical nature most of conventional studies on experimental determining a relationship between burnishing process parameters and treated part properties directly [1–3] or by evaluating their surface layer quality [4–10] has a significant drawback: unsuitability of their results for practical applications in other conditions, that is, for designing new manufacturing processes. More promising approach is to develop analytical techniques of technological support in obtaining given service properties of parts worked out by Smeljansky V.M. [11]. It is based not on external relations of the burnishing parameters but on internal regularities and mechanisms of the surface layer formation in the center of plastic deformation formed on the theoretical basis of continuum mechanics. However, the simplification underlying the analytical dependence of plastic deformation (neglecting the presence in the processed material not only plastic but also elastic deformation the volume of which exceeds that of the plastic deformation) causing lack of sufficient predictive power of this approach.

A number of foreign and domestic publications in recent years (see e.g. [4–6, 8–10]) are devoted to the research of some phenomena to improve the surface quality due to a local elastic-plastic deformation by numerical methods, including finite-element (FE) analysis. This method of continuum mechanics also has reliable theoretical justifica-

tion. Although the FE simulation results are not in sufficiently good agreement with the experimental data, this approach is valuable for understanding the material elastic-plastic behavior in the part surface layers. Obviously, we can solve the urgent problem of engineering techniques for the burnishing prediction by using high-quality numerical models and comprehensive approach to their study.

The aim of this paper is to find out regularities of the elastic-plastic behavior of the plane part material during the indentation by a rigid sphere through creating and studying the FE model, which is a stage of the burnishing process complex research.

The object of the study has been selected due to the followings. Elastic behavior of the materials during the indentation by a spherical indenter investigated correctly by means of elasticity theory. Therefore, it is expected that it will provide a reliable estimation of the model quality for its size, boundary conditions, requirements to the FE size, and the way of the load and restriction applying. It is also suggested that the revealed regularities of stresses and plastic flow during the indentation strengthening will serve as a reliable information base for making up a FE model for revealing peculiarities of similar phenomena in ball burnishing processes and solving the problem of their prediction.

**Building a model and its verification. Study techniques**

It is efficient to simulate the process with the 2D axisymmetrical model in which the sphere is modeled by its thin part adjacent to the contact and the material to be studied by a thick circular plate (Fig. 1). The plate dimensions are many times larger than the largest expected contact. So, in accordance with the Saint-Venant principle, it can be rightly assumed that the restrictions do not affect the stress-strain state of the plate investigated area. The loading is applied by sphere vertical displacement $y$ and indentation force $P$ is defined as the plate reaction at its fixed edges. Such a way of loading provides: an absolute rigidity of the spherical surface, uniquely determines the contact shape, and enables more accurate comparisons of the simulation results with the theoretical data. In addition, the finite elements inside the sphere are practically removed from the analysis saving the calculation time. Contact radius $a$ is determined as $x$ coordinate of the last plate element node pressed by the sphere.

It is known, the less the finite element sizes the higher the FE analysis accuracy but the greater the finite element number, the desired computational resources and time. It has been found by previous studies that about 1% difference between the theoretical data and the simulation results in stress can be achieved if the finite elements size in the plate area adjacent to the contact does not exceed 0,003 mm. In this case, the lowest accuracy (up to 10%) was observed in a detecting contact size $a$ and a location of the plastically deformed areas. Based on the exploratory studies, it was worked out a reasonable mesh model that includes a small area of the plate with small mesh sizes (0,0025 mm) in places where a significant plastic deformation is expected and element sizes of the rest part is very much larger. In order to significantly enhance the simulation accuracy in detecting the contact and plastically deformed areas, element sizes along the expected contact and the contact symmetry axis were gradually decreased in 2–10 times. So the finest mesh was created near the expected contact center.

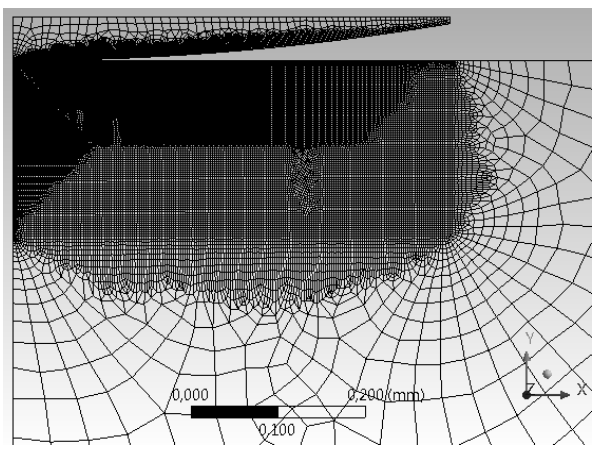

Fig. 1A fine meshed part of the model

The model allows studying the elastic-plastic behavior of any material. Here are the results for the case when the plate material is carbon steel 45 (similar to AISI 1045) with modulus of elasticity, Poisson's ratio and yield strength, respectively $2 \cdot 10^5$ MPa, 0,3, and 350 MPa with a power dependence of isotropic strain strengthening [12]

$$\sigma_{pl} = 350(1 + 0,239\,\varepsilon^{0,48}),$$

where $\varepsilon$ is a degree of deformation, %.

The study showed not only the actual parameters such as indentation force $P$, radius $a$, and contact area $S$, sphere displacement $y$, etc., but also the dimensionless normalized ones (marked with *) with respect to the corresponding values of the same parameters at the moment the plate material is in the very beginning of a plastic flow (marked к$p$): $P^*=P/P_{кр}$, $S^*=S/S_{кр}$, $y^*=y/y_{кр}$. The normalized parameters allow to make many simulating results to be invariant to the model geometrical and mechanical particular parameters.

Since the plate material while indenting the sphere expected to be in a complex stress state, the condition of a plastic flow in the material according to the von Mises criterion is

$$\sigma_{кр}=\sqrt{\tfrac{1}{2}((\sigma_1-\sigma_2)^2+(\sigma_2-\sigma_3)^2+(\sigma_3-\sigma_1)^2}, \quad (1)$$

where $\sigma_i$, ($i$=1, 2, 3) is the principal stresses in a complex stress state; $\sigma_{kr}$ is a yield stress of the material in a simple tension.

The expression of the right side of equation (1) is equivalent stress $\sigma_{eq}$ or the von Mises stress.

The model quality was tested by comparing the results of the numerical and theoretical modeling (by the Hertz theory [13]) for normalized displacement $y^*$ (8 points) with its variation ranges from 0,5 to 1. An average error for maximum pressure $\sigma_3$ in the contact center was 0,25% with a standard deviation of 0,0295. The comparison results for indentation parameters which are independent of the sphere displacement by the Hertz theory are summarized in the table. The results confirm the high accuracy for stresses evaluated by the FE model.

**FE Simulation results and their analysis**

The modeling studies have shown that the development of the plate stress-strain state during the sphere indentation can be divided into two stages:

1. The elastic stage which lasts from the very beginning of the sphere indentation until gaining the critical stress by the expression (1) in the plate most severely stressed point. The elastic state is observed at y*≤1 (Fig. 2,*a*,*b*);

2. The elastic-plastic stage (y*>1) happens when the stress in any part of the plate material reaches or exceeds the critical value and a plastic flow occurs. The rest of the material is in an elastic state.

The elastic-plastic stage develops in three phases.

**T a b l e**. Comparison of the sphere indentation parameters for the plate elastic state by the Hertz theory and the FE simulation

| Comparison factor | $h/a$ | $\sigma_{\tau\,max}/\sigma_3$ | $\sigma_{eq.max}/\sigma_{\tau\,max}$ | $\sigma_1/\sigma_3=\sigma_2/\sigma_3$ |
|---|---|---|---|---|
| The theoretical results | 0,48 | 0,31 | 2 | approximately 0,8 |
| Average FE simulation results $R$ | 0,480 | 0,309 | 2,00 | 0,796 |
| Standard deviations $Sd$ of FE simulation results | 0,0078 | 0,0002 | 0,00005 | 0,0002 |
| Relative standard deviations $Sd/R$, % | 1,63 | 0,06 | 0,003 | 0,03 |
| Deviations from the theoretical results, % | 0,0 | 0,32 | 0,0 | approximately 0,5 |
| *Notes:* $h$ is a depth of the maximum equivalent $\sigma_{eq.max}$ and shear $\sigma_{\tau.max}$stresses; $\sigma_i$, ($i$=1,2,3)is principal stresses in the contact center | | | | |

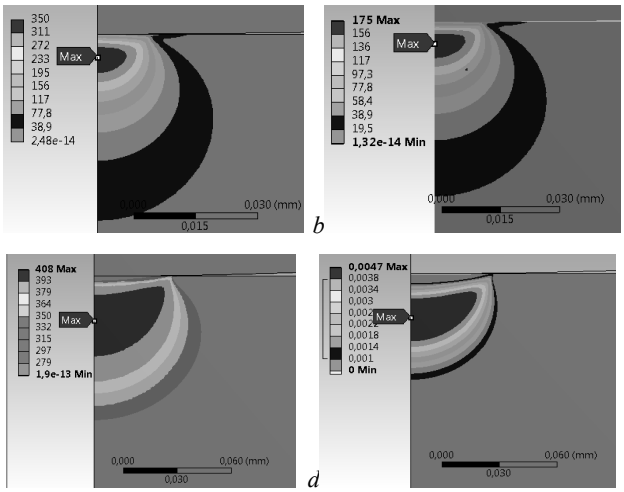


Fig. 2. Distribution of equivalent (a) and intensity (b) stresses in the plate ($y^*$=1, the elastic stage), and equivalent stress (c) and plastic deformation (d) for $y^*$=10 (the first phase of the elastic-plastic stage)

In the first phase (1<$y^*$<15), the plastic material area is completely surrounded by the material in an elastic state (Fig. 2,*c*,*d*). The material strengthening the flows so that the maximum equivalent stress, stress intensity (like in the elastic stage (Fig. 2,*a*,*b*)), and the maximum equivalent plastic strain are located on the contact symmetry axis at the same depth $h$ from the contact center. The increase in relative depth $h/a$ (maximum stresses and plastic strain placement on the contact vertical symmetry axis (Fig. 3)) indicates the prevailing development of material strengthening in a depth. However, the material plastic flow causes the stress leveling in the radial direction both in the plate volume and in its contact. So, the maximum contact pressure gradually shifts from the contact center to its periphery (relative coordinate $x/a$ of its applying increases,

see Fig. 4, plot *x_P*max_*a*) and the pressure distribution in the contact (coefficient *K* of pressure distribution – ratio of maximum pressure $P_{max}$ in the contact and average pressure *P/S* – reduces, see Fig. 4, plot *K*) levels as well. Note that for the elastic state ($y^* \le 1$), *K* is close to 1,5 which corresponds to the contact pressure distribution by a hemisphere; if the distribution is uniform *K*=1.

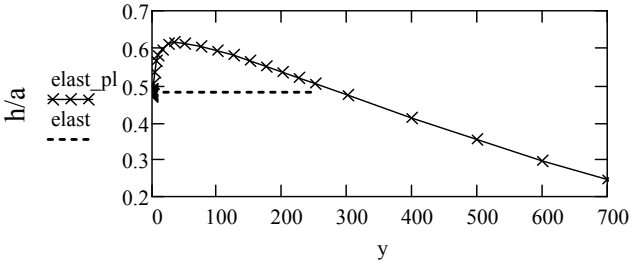


Fig. 3. Relative location *h*/*a* of the maximum equivalent stress and stress intensity on the contact symmetry axis versus $y^*$ for the material states: elastic-plastic (plot «elast_pl»), idealized elastic (plot «elast»)

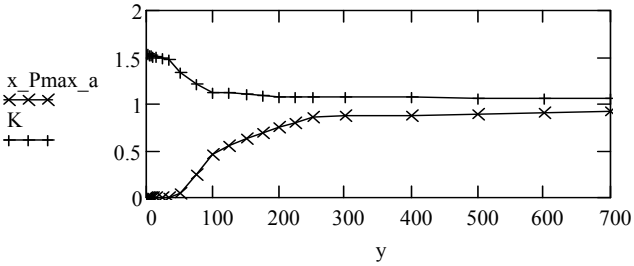


Fig. 4. Relative radius *x*/*a* (plot «x_*P*max_a») applying maximum contact pressure $P_{max}$ and K versus $y^*$

An important feature of the second phase of the material elastic-plastic behavior ($15 \le y^* < 50$) is the critical stress yields up to the contact surface and spreads to its center. The phase is characterized by the followings: a practical stability and the largest values of ratio *h/a* (Fig. 3), leveling off the stress and consequently the plastic deformation along some curve toward the edge of the plastically deformed contact (Fig. 5, $y^*$=15 and 35).Their difference is less than 1%. Such behavior of the stress-strain state is associated with leveling off the contact pressure and increasing coordinate *x/a* applying maximum pressure $P_{max}$ (see Fig. 4).

The results of the material elastic-plastic behavior under the spherical indenter and regularities of its strain strengthening make it possible to choose a reasonably rational option range for further 3D FE research of a ball burnishing process. This will facilitate the research and improve the result reliability. Such studies should be performed in the range of ball normalized displacement $y^*$ from 35 to 150, i.e., within parts of the second and third phases of the material elastic-plastic stage.

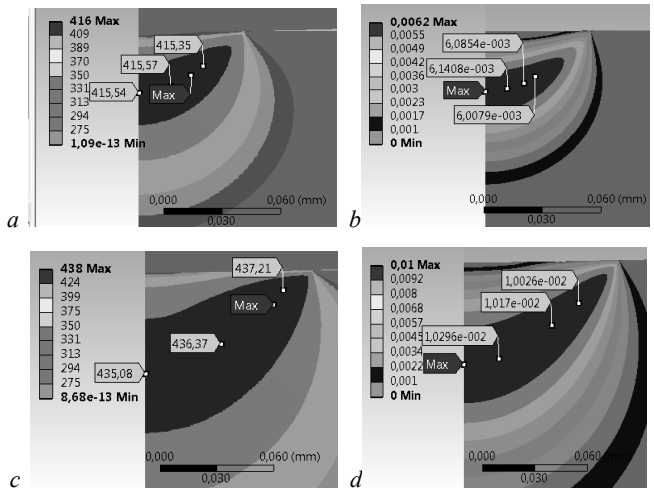


Fig. 5. Distribution of equivalent stress (*a*,*c*) and plastic deformation (*b*,*d*) for the second phase of the elastic-plastic stage: $y^*$=15 (*a*,*b*); $y^*$=35 (*c*,*d*)

The third phase ($y^* \ge 50$) begins with the completion of the continuous plastic state formation of the material in the contact – the critical stress reaches its center. In this case, the contact is increasing more intensively (decreasing ratio *h/a*, see Fig. 3) with practically a constant rate. An overall depth and width of the material plastically deformed area increase significantly (Fig. 6). Moreover, it extends beyond the contact edge ($y^* > 150$, see Fig. 7,*d*,*e*,*i*,*j*) forming a projecting collar.

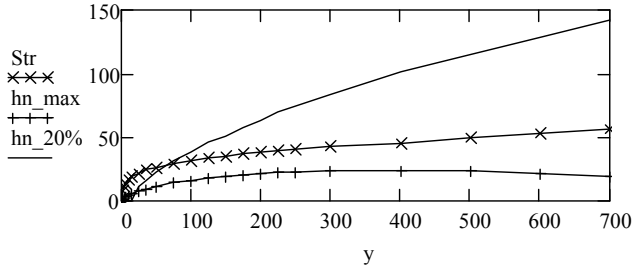


Fig. 6. The material maximum strengthening (chart «Str», %), its depth $h/h_{kr}$ (plot «*hn*_max») and depth of 20% strengthening $h_{20}/h_{kr}$ (plot «hn_20 %») at the contact symmetry axis versus $y^*$

This range of the indenter displacement is inherent in: a high level of material strengthening – from 24 to 35%, a high degree of uniformity in the distribution of the strengthened region (see Fig. 5 and 7), a significant depth and width of the plastically deformed area is approximately equal to the contact size. Furthermore, we should expect a high sta-

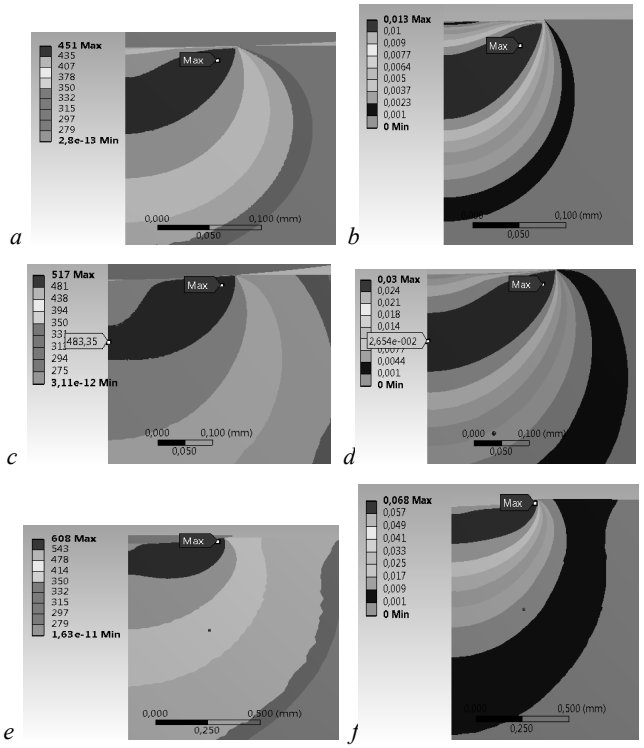


Fig. 7. Distribution of equivalent stress (*a*,*c*,*e*) and plastic deformation (*b*,*d*,*f*) for the third phase of the elastic-plastic stage: $y^*$=50 (*a*,*b*); $y^*$=200 (*c*,*d*); $y^*$=700 (*c*,*d*)

bility of the process due to a small dependence $h/a$ from $y^*$ for this range (see Fig. 3).The upper limit of the recommended range is selected base on the fact that when $y^*>150$ plastically deformed material extends beyond the contact to form a collar of plastically strengthened material. Its appearance may cause some unwanted effects: instability of the process and results of the material strengthening along the feed direction through successive increasing in the collar height and related changes in burnishing geometry and forces; an excessive material plastic deformation can cause its destruction; an appearance of great waviness on machined surfaces that will require an additional grinding operation.

**Conclusions**

This paper shows a feasibility of using finite element analysis to study burnishing processes of the machine part surfaces. The FE model has been created for simulating a rigid sphere indentation in a half-space for a wide range of the sphere normalized displacement. Its good quality is confirmed by the Hertz contact theory for ball elastic indentation into a flat surface. The model simulation of the material behavior with a power dependence of isotropic strain strengthening revealed that the stage of an elastic-plastic deformation proceeds three phases, which differ in the stresses and strains distribution in the volume, contact, and surfaces around it. The revealed regularities helped to justify a reasonable range of the ball displacement variation for further FE studying ball burnishing processes. Such studies should be performed in the range of ball displacement $y^*$ from 35 to 150.


1. *Одинцов Л.Г.* Упрочнение и отделка деталей поверхностным пластическим деформированием: Справочник. – М.: Машиностроение, 1987. – 328 с.
2. *Папшев Д.Д.* Отделочно-упрочняющая обработка поверхностным пластическим деформированием. – Там же, 1978. – 152 с.
3. *Пшибыльский В.* Технология поверхностной пластической обработки. – М.: Металлургия, 1991. – 479 с.
4. *Тітов А.В.* Формування поверхневого шару деталей вигладжуванням для підвищення їх ресурсу // Автореф. дис. … канд. техн. наук. – К.: НТУ «КПІ», 2007. – 24 с.
5. *Сидякин Ю.И.* Разработка метода расчета упругопластических контактных деформаций в процессах упрочнения деталей поверхностным пластическим деформированием: Автореф. дис. … д-ра. техн. наук. – Волгоград: ВолгГТУ, 2002. – 42 с.
6. *Лях В.*, *Андрущенко В.* Вивчення пружно-пластичної поведінки матеріалів при мікроіндентуванні сферичним індентором // Вісн. Київськ. нац. ун-ту імені Тараса Шевченка, Математика. Механіка. – К.: КНУ, 2010. – **24**. –С. 47–49.
7. *Dj. Vukelic1* A burnishing process based on the optimal depth of workpiece penetration // Materials and technology. – 2013. – **47**, N 1. – P. 43–51.
8. *Deepak Mahajan*, *Ravindra Tajane*. A Review on Ball Burnishing Process// Int. J. of Scientific and Research Publications. – 2013. – **3**, Issue 4. – P. 1–8.
9. *Sayahi M.*, *Sghaier S.*, *Belhadjsalah H.* Finite element analysis of ball burnishing process: comparisons between numerical results and experiments // Int. J. of Advanced Manufacturing Technology. – 2013. – **67**, Issue 5-8. – P 1665–1673.
10. *Ghodake A. P.*, *Rakhade R.D.*, *Maheshwari A.S.* Effect of Burnishing Process on Behavior of Engineering Materials // A Review.. J. of Mechanical and Civil Engineering. – 2013. – **5**, Issue 5. – P. 09–20.
11. Смелянский В.М. Механика упрочнения деталей поверхностным пластическим деформированием. – М.: Машиностроение, 2002. – 300 с.
12. *Третьяков А.В.*, *Трофимов Г.К.*, *Гурьянова М.К.* Механические свойства сталей и сплавов при пластическом деформировании: Справочник. – М.: Машиностроение, 1971. – 63 с.
13. *Писаренко Г.С.*, *Квітка О.Л.*, *Уманський Е.С.* Опір матеріалів: Підручник – К.: Вища шк., 2004. – 655 с.


Поступила 09.04.2015
*E-mail*: *leuro@list.ru*